J. Phys. G: Nucl. Part. Phys. **16** (1990) 395–415. Printed in the UK

Comparison of quantised ATDHF and GCM theory with application to the $^{12}C + ^{20}Ne$ system

B Slavov§, F Grümmer†, K Goeke†, R Gissler‡,
V I Dimitrov‡§ and Ts Venkova‡||

† Institut für Theoretische Physik II, Ruhr-Universität Bochum, D-4630 Bochum, Federal Republic of Germany

‡ Institut für Kernphysik, Kernforschungsanlage Jülich, D-5170 Jülich, Federal Republic of Germany

Received 20 September 1989

Abstract. A conceptional and numerical comparison of one parameter generator coordinate method (GCM) and quantised adiabatic time-dependent Hartree–Fock (ATDHF) theory is performed by applying both theories to the $^{12}C + ^{20}Ne$ and $^{16}O + ^{16}O$ system. Different parametrisations of the Skyrme interaction are used. The single-particle wavefunctions and the operators are represented on a three-dimensional grid in coordinate and momentum space. The collective path is evaluated in the gradient method, corresponding to GCM, and by solving the numerically more involved ATDHF equations. The potential, translational and rotational moments of inertia are calculated along these collective paths as well as the mass parameters corresponding to relative motion. As the next step, the quantised collective Hamiltonian is extracted from the collective path and subbarrier fusion cross sections, as well as astrophysical S factors, are calculated by means of generalised WKB techniques. This allows discussion of the differences between the various methods at a significant and sensitive physical quantity. Whereas for the doubly closed system $^{16}O + ^{16}O$ the GCM turns out to be a rather good approximation to quantised ATDHF, there are significant differences in the doubly open $^{12}C + ^{20}Ne$ system.

1. Introduction

For the description of large-amplitude nuclear collective motion such as subbarrier fusion and fission there basically exist, besides the path integral approaches, two kinds of quantum-mechanical and microscopic theories: GCM-like theories and adiabatic theories, such as e.g. quantised ATDHF. Both approaches are approved in realistic applications to heavy-ion systems (Friedrich *et al* 1974, Fiebig and Weiguny 1976, Goeke *et al* 1983, Provoost *et al* 1984). They allow for the evaluation of the motion by means of a collective Hamiltonian in terms of mass parameters, collective potentials, quantum corrections and the centrifugal force. However, it is known that in both models these quantities are not identical. It is further known, and will be

§ Permanent address: Faculty of Physics, Sofia University, 1126 Sofia, Bulgaria.

|| Permanent address: Bulgarian Academy of Sciences, Institute for Nuclear Research and Nuclear Energy, 1784 Sofia, Bulgaria.

0954-3899/90/030395 + 21 $03.50

recalled in §2, that the GCM (in the Gaussian overlap approximation) is an approximation to quantised ATDHF. It is an aim of this paper to investigate the differences numerically for a realistic heavy-ion collision. Both theories use as the basic ingredient a collective path ($|\phi_q\rangle$) which manifests changes of the structure of the system during the collision. The quantised ATDHF provides a clear prescription for the choice of the collective path and yields asymptotically correct masses (Goeke *et al* 1983). However, the numerical procedure for solving the ATDHF equation is time consuming; therefore, the question arises as to whether it is worthwhile to apply such a considerable amount of effort. In order to investigate this we discuss besides the ATDHF-path the collective path of the gradient method, obtained by means of the GCM theory (Goeke and Reinhard 1980). Its calculation takes about 15% of the computer time required to evaluate the full ATDHF path. The comparison of the potentials and mass parameters along the collective paths is performed for the ^{12}C–^{20}Ne system. This system is chosen because it represents a rather general case due to its deformed non-closed shells. In order to obtain reliable results we employ the usual and well established Skyrme interactions and perform the calculations on a three-dimensional grid in coordinate and momentum space.

To exemplify the various prescriptions to obtain collective masses, potentials etc, we calculate as a relevant physical quantity the subbarrier fusion cross section of $^{12}C + {}^{20}Ne \rightarrow {}^{32}S$. We show that for such a system the use of GCM as an approximation to quantised ATDHF is not justified, in contrast to a doubly closed system as $^{16}O + {}^{16}O$.

In §§2.1 and 2.2 we briefly review the main concepts of one-parameter GCM and of quantised ATDHF theory. Section 3 reviews shortly the formulation of the theory with the Skyrme interactions. In §4 we demonstrate the conceptional differences and the relations of GCM and ATDHF mass parameters. Section 5 considers the numerical techniques used, especially for the evaluation of the self consistent Thouless–Valatin mass. The application to the ^{12}C–^{20}Ne system is presented in §6. Finally, some conclusions are given in §7.

2. Theory of GCM and quantised ATDHF

In this section we review the basic concepts and formulae of GCM and quantised ATDHF as far as it is needed for the present considerations. The details of GCM can be found in Fiebig *et al* (1976), Friedrich *et al* (1974, 1981), Deumens (1982), Ring and Schuck (1980), and those of quantised ATDHF in Goeke and Reinhard (1980), Goeke *et al* (1983), Reinhard and Goeke (1987).

2.1. The GCM theory

In the usual formulation of the one-parameter GCM theory (Ring and Schuck 1980) one diagonalises the total Hamiltonian H in the subspace spanned by the Slater determinants of the collective path. These Slater determinants $|\phi_q\rangle$ are time-even functions and they depend just on one real coordinate, q. The stationary wave function of the A-body system is then given as a linear superposition of the $|\phi_q\rangle$

$$\psi^{\mathrm{GCM}} = \int \mathrm{d}q f(q) |\phi_q\rangle. \tag{2.1}$$

In Reinhard and Goeke (1979), the collective path $|\phi_q\rangle$ and the weight function $f(q)$ are determined by a double variational method requiring that the expectation value of the energy in the state $|\psi^{\mathrm{GCM}}\rangle$ is stationary with respect to variations of $f(q)$ and $|\phi_q\rangle$

$$\delta \langle \psi^{\mathrm{GCM}}| H - E |\psi^{\mathrm{GCM}}\rangle = 0. \tag{2.2}$$

The variation is performed in the Gaussian overlap approximation (GOA) for the overlap kernels of the norm and of the Hamiltonian. The variation with respect to $|\phi_q\rangle$ yields, assuming adiabatic motion (Reinhard and Goeke 1979)

$$\delta \langle \phi_q| H - \frac{\partial V}{\partial q}\frac{\partial}{\partial q}|\phi_q\rangle = 0. \tag{2.3}$$

The solution of this variational principle leads to the non-linear differential equation

$$\frac{\partial}{\partial q}|\phi_q\rangle = \left(\frac{\partial V}{\partial q}\right)^{-1} H_{\mathrm{ph}}|\phi_q\rangle. \tag{2.3a}$$

If one transforms this differential equation to a difference equation with a finite step ε_{G} one obtains

$$|\phi_{q_{n+1}}\rangle = (1 - \varepsilon_{\mathrm{G}} H_{\mathrm{ph}})|\phi_{q_n}\rangle \tag{2.4}$$

where H_{ph} is the 1p–1h and 1h–1p part of the total Hamiltonian H. This procedure is called gradient method (GRAD). The 1p–1h and 1h–1p matrix elements are to be taken with respect to $|\phi_q\rangle$ and $|\phi_{q_n}\rangle$, respectively.

The collective Hamiltonian is obtained by variation of (2.2) with respect to the weight function $f(q)$. The result is an integral equation, the so called Hill–Wheeler equation (Hill and Wheeler 1953, Griffin and Wheeler 1957). It can be transformed into a differential equation, the collective Schrödinger equation (Goeke and Reinhard 1980)

$$H_{\mathrm{C}}^{\mathrm{GCM}}\left(q, \mathrm{i}\hbar\frac{\mathrm{d}}{\mathrm{d}q}\right) g(q) = E g(q) \tag{2.5a}$$

where

$$g(q) = \int \mathrm{d}q' [\phi_q, \phi_{q'}]^{1/2} f(q'). \tag{2.5b}$$

In case of, e.g., a heavy-ion collision, where q is conveniently chosen to describe the distance between the fragments, one deals with deformed states and has therefore to consider the rotation of the system. In the GOA this can be taken into account by proper zero point energies and centrifugal terms. If one, in addition, also considers spurious translations one obtains altogether the following form for the collective Hamiltonian in case of axially symmetric wavefunctions (Goeke *et al* 1983)

$$\begin{aligned} H_{\mathrm{C}}^{\mathrm{GCM}}&\left(q, \mathrm{i}\hbar\frac{\mathrm{d}}{\mathrm{d}q}\right) \\ &= -\frac{1}{4}\left(\frac{\mathrm{d}^2}{\mathrm{d}q^2}\frac{\hbar^2}{2M^{\mathrm{GCM}}(q)} + \frac{\mathrm{d}}{\mathrm{d}q}\frac{\hbar^2}{M^{\mathrm{GCM}}(q)}\frac{\mathrm{d}}{\mathrm{d}q}\right. \\ &\quad \left. + \frac{\hbar^2}{2M^{\mathrm{GCM}}(q)}\frac{\mathrm{d}^2}{\mathrm{d}q^2}\right) \\ &\quad + V(q) - Z^{\mathrm{GCM}}(q) + \frac{\hbar^2}{2\theta^{\mathrm{GCM}}(q)} L(L+1). \end{aligned} \tag{2.6}$$

The collective mass parameter is given by

$$\frac{1}{M^{\mathrm{GCM}}(q)} = \frac{\langle \phi_q | \{P, \{\bar{H}, P\}\} | \phi_q \rangle}{4 \langle \phi_q | P^2 | \phi_q \rangle^2} \tag{2.7}$$

with $\bar{H} = H - \langle \phi_q | H | \phi_q \rangle$ and

$$P | \phi_q \rangle = \mathrm{i}\hbar \frac{\partial}{\partial q} | \phi_q \rangle. \tag{2.8}$$

The $V(q)$ is the classical potential, defined by

$$V(q) = \langle \phi_q | H | \phi_q \rangle. \tag{2.9}$$

The $Z(q)$ accounts for the quantum corrections which include the kinetic and potential zero-point energies along the collective path and an approximate projection on angular momentum $L = 0$ and translational momentum $k = 0$

$$Z^{\mathrm{GCM}}(q) = Z^{\mathrm{GCM}}_{\mathrm{kin}}(q) + Z^{\mathrm{GCM}}_{\mathrm{pot}}(q) + Z^{\mathrm{GCM}}_{\mathrm{rot}}(q) + Z^{\mathrm{GCM}}_{\mathrm{trans}}(q) \tag{2.10}$$

with

$$Z^{\mathrm{GCM}}_{\mathrm{kin}}(q) = \frac{\hbar^2}{2M^{\mathrm{GCM}}(q)} \langle \phi_q | \frac{\vec{\partial}}{\partial q} \frac{\vec{\partial}}{\partial q} | \phi_q \rangle \tag{2.11}$$

$$Z^{\mathrm{GCM}}_{\mathrm{pot}}(q) = \frac{1}{8 \langle \phi_q | P^2 | \phi_q \rangle} \frac{\partial^2 V}{\partial q^2} \tag{2.12}$$

$$Z^{\mathrm{GCM}}_{\mathrm{rot}}(q) = \sum_{i=1}^{3} \frac{\hbar^2}{2\theta_i^{\mathrm{GCM}}(q)} \langle \phi_q | (J^{(i)}_{\mathrm{ph}})^2 | \phi_q \rangle \tag{2.13}$$

$$Z^{\mathrm{GCM}}_{\mathrm{trans}}(q) = \sum_{i=1}^{3} \frac{\hbar^2}{2M_i^{\mathrm{GCM}}(q)} \langle \phi_q | \vec{\nabla}^{(i)}_{\mathrm{ph}} \vec{\nabla}^{(i)}_{\mathrm{ph}} | \phi_q \rangle. \tag{2.14}$$

The translational and rotational moments of inertia, M_i^{GCM} and θ_i^{GCM} are consistently to be calculated in the Peierls–Yoccoz (Peierls and Yoccoz 1957) approximation. This corresponds to the GCM approximation (2.7). It is a drawback of the one parameter GCM that its mass parameter does not yield the correct values $M = mA$ for a pure translational of the A-body system and $M = \mu$ (reduced mass) for a pure relative motion. Moreover the collective gradient-path is not maximally decoupled. Both disadvantages are avoided in quantised ATDHF theory.

2.2. *The quantised ATDHF theory*

The stationary wavefunction $|\psi^{\mathrm{ATDHF}}\rangle$ is built up by a linear superposition of Slater determinants $|\phi_{qp}\rangle$ labelled by a pair of conjugate collective parameters q and p rather than by a single parameter as in GCM

$$|\psi^{\mathrm{ATDHF}}\rangle = \int \mathrm{d}q \, \mathrm{d}p f(q,p) \, |\phi_{qp}\rangle. \tag{2.15}$$

In the adiabatic approximation one writes the Slater determinants as follows

$$|\phi_{qp}\rangle = [1 + \mathrm{i}pQ(q)] \, |\phi_q\rangle \tag{2.16}$$

where the $|\phi_q\rangle$ are time-even Slater determinants and Q is a Hermitian and time-even 1p–1h operator.

Similarly to the case of one parameter GCM the collective path $|\phi_q\rangle$, the $Q(q)$ and the weight function $f(q,p)$ are determined by requiring (Reinhard and Goeke 1979, Goeke and Reinhard 1980) that the expectation value of the energy is stationary with respect to variations of $|\phi_q\rangle$ and $f(q,p)$

$$\delta \langle \psi^{\mathrm{ATDHF}}| H - E |\psi^{\mathrm{ATDHF}}\rangle = 0. \tag{2.17}$$

The variation with respect to $|\phi_q\rangle$ yields

$$\delta \langle \phi_q| H - \frac{\partial V}{\partial q} Q |\phi_q\rangle = 0 \tag{2.18}$$

$$\delta \langle \phi_q| [H, Q] + \frac{\mathrm{i}\hbar}{M^{\mathrm{ATDHF}}(q)} P |\phi_q\rangle = 0 \tag{2.19}$$

with the Hermitian and time odd 1p–1h operator P given as

$$P |\phi_q\rangle = \mathrm{i}\hbar\, \partial_q |\phi_q\rangle \tag{2.20}$$

where the particles and holes are those of $|\phi_q\rangle$. The Q and P are normalised such that

$$\langle \phi_q| [Q, P] |\phi_q\rangle = \mathrm{i}\hbar. \tag{2.21}$$

The classical potential $V(q)$ is defined by

$$V(q) = \langle \phi_q| H |\phi_q\rangle \tag{2.22}$$

and the ATDHF mass parameter M^{ATDHF} is given by

$$\frac{\hbar^2}{M^{\mathrm{ATDHF}}(q)} = \langle \phi_q| [Q, [H, Q]] |\phi_q\rangle. \tag{2.23}$$

The ATDHF equations (2.18) and (2.19) can be reformulated as a single non-linear differential equation of first order in q

$$\frac{\partial}{\partial q} |\phi_q\rangle = c(q)[H, H_{\mathrm{ph}}]_{\mathrm{ph}} |\phi_q\rangle \tag{2.24}$$

with

$$c(q) = \left(\frac{\partial V}{\partial q}\right)^{-1} \frac{M^{\mathrm{ATDHF}}(q)}{\hbar^2}. \tag{2.25}$$

The Q can be expressed in terms of H_{ph}

$$Q = \left(\frac{\partial V}{\partial q}\right)^{-1} H_{\mathrm{ph}}. \tag{2.26}$$

Here H_{ph} is again the 1p–1h + 1h–1p part of the Hamiltonian with respect to $|\phi_q\rangle$.

The differential equation (2.24) needs an initial condition. This is obtained by requiring minimal coupling of the collective degrees of freedom to the intrinsic ones. The degree of coupling is determined by the validity condition (Slavov *et al* 1986). By experience it is known (Goeke *et al* 1983) that the collective path starting at a saddle point is the optimal one, showing minimal coupling. Then, (2.24) is solved by

finite steps choosing $\delta qc(q) = -\varepsilon_A$ which yields the following equation for the ATDHF path

$$|\phi_{q_{n+1}}\rangle = (1 - \varepsilon_A[\mathrm{H}, \mathrm{H}_{\mathrm{ph}}^{(n)}]_{\mathrm{ph}}^{(n)})\,|\phi_{q_n}\rangle. \tag{2.27}$$

This equation is to be contrasted with the corresponding (2.4) of the GRAD method. Apparently the operations in (2.27) are more complicated and in addition the $\varepsilon_A \ll \varepsilon_G$. Thus the evaluation of the ATDHF path takes about an order of magnitude more computer time. By variation of (2.17) with respect to $f(q,p)$ we obtain the Hill–Wheeler equation for $f(q,p)$. Due to the properties of the ATDHF path this can be transformed (Goeke and Reinhard 1980) to a collective Schrödinger equation solely in q

$$H_{C,L}^{\mathrm{ATDHF}}\left(q, \mathrm{i}\hbar\frac{\mathrm{d}}{\mathrm{d}q}\right)g(q) = Eg(q). \tag{2.28}$$

with

$$\begin{aligned} H_{C,L}^{\mathrm{ATDHF}}&\left(q, \mathrm{i}\hbar\frac{\mathrm{d}}{\mathrm{d}q}\right) \\ &= -\frac{1}{4}\left(\frac{\mathrm{d}^2}{\mathrm{d}q^2}\frac{\hbar^2}{2M^{\mathrm{ATDHF}}(q)} + \frac{\mathrm{d}}{\mathrm{d}q}\frac{\hbar^2}{M^{\mathrm{ATDHF}}(q)}\frac{\mathrm{d}}{\mathrm{d}q}\right. \\ &\quad \left. + \frac{\hbar^2}{2M^{\mathrm{ATDHF}}(q)}\frac{\mathrm{d}^2}{\mathrm{d}q^2}\right) \\ &\quad + V(q) - Z^{\mathrm{ATDHF}}(q) + \frac{\hbar^2}{2\theta^{\mathrm{ATDHF}}(q)}L(L+1). \end{aligned} \tag{2.29}$$

Concerning the zero-point energies and the centrifugal term we proceeded in analogy to the GCM theory in §2.1, $g(q)$ being given by (2.5*b*).

Again, the $Z(q)$ accounts for the quantum corrections which include the kinetic and potential zero-point energies along the collective path and an approximate projection on angular momentum $L = 0$ and translational momentum $k = 0$

$$Z^{\mathrm{ATDHF}}(q) = Z_{\mathrm{kin}}^{\mathrm{ATDHF}}(q) + Z_{\mathrm{pot}}^{\mathrm{ATDHF}}(q) + Z_{\mathrm{rot}}^{\mathrm{ATDHF}}(q) + Z_{\mathrm{trans}}^{\mathrm{ATDHF}}(q) \tag{2.30}$$

with

$$Z_{\mathrm{kin}}^{\mathrm{ATDHF}}(q) = \frac{\hbar^2}{2M^{\mathrm{ATDHF}}(q)}\langle\phi_q|\frac{\overleftarrow{\partial}}{\partial q}\frac{\vec{\partial}}{\partial q}|\phi_q\rangle \tag{2.31}$$

$$Z_{\mathrm{pot}}^{\mathrm{ATDHF}}(q) = \tfrac{1}{2}\langle\phi_q|Q^2|\phi_q\rangle\frac{\partial^2 V}{\partial q^2} \tag{2.32}$$

$$Z_{\mathrm{rot}}^{\mathrm{ATDHF}}(q) = \sum_{i=1}^{3}\frac{\hbar^2}{2\theta_i^{\mathrm{ATDHF}}(q)}\langle\phi_q|(J_{\mathrm{ph}}^{(i)})^2|\phi_q\rangle \tag{2.33}$$

$$Z_{\mathrm{trans}}^{\mathrm{ATDHF}}(q) = \sum_{i=1}^{3}\frac{\hbar^2}{2M_i^{\mathrm{ATDHF}}(q)}\langle\phi_q|\vec{\nabla}_{\mathrm{ph}}^{(i)}\vec{\nabla}_{\mathrm{ph}}^{(i)}|\phi_q\rangle. \tag{2.34}$$

Here the ATDHF prescription for the translational and rotational inertia parameters corresponds to a simple generalisation of the Thouless–Valatin formula to non-equilibrium states. We present in §4, how the masses will be evaluated.

If one compares the formulae of §2.1 with those of §2.2 one realises clearly that GCM with Gaussian overlaps and using one collective parameter is an approximation to quantised ATDHF using a pair of conjugate parameters.

3. The GRAD and ATDHF path with the Skyrme interaction

According to the Thouless theorem equations (2.4) for the gradient path and (2.27) for the ATDHF path can be written in terms of the single-particle wavefunctions $|\alpha\rangle$ with $\alpha = 1, \ldots, A$. Furthermore, the operator H_{ph} and the commutator $[H, H_{\text{ph}}]_{\text{ph}}$ can be expressed (Goeke *et al* 1983) by the Hartree–Fock Hamiltonian W_0 and the linear response operator W_1. This then reads for the gradient path

$$|\alpha, n+1\rangle = \{1 - \varepsilon_G(1-\rho_0)W_0\}\,|\alpha, n\rangle \tag{3.1}$$

and for the ATDHF path

$$|\alpha, n+1\rangle = \{1 - \varepsilon_A(1-\rho_0)[W_0(1-2\rho_0)W_0 + W_1]\}\,|\alpha, n\rangle \tag{3.2}$$

where the index n indicates the nth iteration step. Here the single-particle density matrix is given by (omitting the index n)

$$\rho_0 = \sum_{\alpha=1}^{A} |\alpha\rangle\,\langle\alpha|. \tag{3.3}$$

The Hartree–Fock Hamiltonian W_0 is

$$W_0 = T + \text{Tr}\{\rho_0 v\}. \tag{3.4}$$

with the effective two-body interaction v. The operator W_1 is given by

$$W_1 = \text{Tr}\{v[W_0, \rho_0]\}. \tag{3.5}$$

W_0 and W_1 depend on the effective interaction. We use for our calculations the Skyrme force without the *ls* coupling term and with a direct Coulomb force. In the special case of spin-saturated and charge-conjugated nuclei we obtain the following expressions for W_0 and W_1 (Engel *et al* 1975)

$$W_0 = -\nabla\left(\frac{\hbar^2}{2m} + \frac{(3t_1+5t_2)}{16}\rho_0(\boldsymbol{r})\right)\nabla + \tfrac{3}{4}t_0\rho_0(\boldsymbol{r}) + \frac{(3t_1+5t_2)}{16}\tau_0(\boldsymbol{r}) - \frac{(9t_1-5t_2)}{32}(\nabla^2\rho_0(\boldsymbol{r})) + \frac{(2+\alpha)}{16}t_3\rho^{1+\alpha}(\boldsymbol{r}) + \tfrac{1}{4}e^2\int \mathrm{d}^3r'\,\frac{\rho_0(\boldsymbol{r}')}{|\boldsymbol{r}-\boldsymbol{r}'|}. \tag{3.6}$$

The kinetic-energy density $\tau_0(\boldsymbol{r})$ is given by

$$\tau_0(\boldsymbol{r}) = [\nabla \cdot \nabla'\rho_0(\boldsymbol{r}, \boldsymbol{r}')]_{\boldsymbol{r}=\boldsymbol{r}'} \tag{3.7}$$

and W_1 is

$$W_1 = \frac{(3t_1+5t_2)}{32}[\nabla \cdot \boldsymbol{j}(\boldsymbol{r}) + \boldsymbol{j}(\boldsymbol{r}) \cdot \nabla] \tag{3.8}$$

where the current density $\boldsymbol{j}(\boldsymbol{r})$ is given by

$$\boldsymbol{j}(\boldsymbol{r}) = [(\nabla - \nabla')\rho_1(\boldsymbol{r}, \boldsymbol{r}')]_{\boldsymbol{r}=\boldsymbol{r}'}. \tag{3.9}$$

Table 1. The parameters of the Skyrme interactions and the ratio m^*/m.

	SK V	SK III	SK M*	SK BKN
α	1.0	1.0	1/6	1.0
t_0(MeV fm^3)	−1248.29	−1128.75	−2645.0	−1089.0
t_1(MeV fm^5)	970.56	395.0	410.0	251.11
t_2(MeV fm^5)	107.22	−95.0	135.0	−150.66
t_3(MeV fm^6)	0.0	14000.0	15595.0	17270.0
m^*/m	0.38	0.76	0.79	1.0

Here $\rho_1(\boldsymbol{r}, \boldsymbol{r}')$ is defined as

$$\rho_1(\boldsymbol{r}, \boldsymbol{r}') = \sum_{\alpha=1}^{A} \{\langle \boldsymbol{r}| (W_0)_{\text{ph}} |\alpha\rangle\langle\alpha | \boldsymbol{r}'\rangle - \langle \boldsymbol{r} | \alpha\rangle\langle\alpha | (W_0)_{\text{ph}} |\boldsymbol{r}'\rangle\}. \tag{3.10}$$

t_0, t_1, t_2, t_3 and α are the parameters of the Skyrme interaction. We use for our calculations the parameterisations SK III and SK V (Beiner *et al* 1975), and in some cases also SK BKN and SK M*. The parameters and the ratio m^*/m are given in table 1.

The parametrisation SK BKN was obtained by Bonche *et al* (1976) by readjusting the parameters of SK VI in order to get $m^*/m = 1.0$. The parametrisation SK M* was adapted by Bartel *et al* (1982), to binding energies, surface properties and fission barriers. It is important to notice that for the interaction SK BKN with $m^*/m = 1$ the operator W_1 vanishes.

4. Mass parameters and linear response

As in the case of the collective ATDHF mass for the relative motion we obtain the ATDHF inertia parameters for translation and rotation by determining the appropriate linear response operators. This can be done at any $|\phi_q\rangle$. However, for simplicity we drop the coordinate q in the following. Of course the resulting inertia parameter will depend on q. As an example, the linear response operators to

$$P|\phi\rangle = \mathrm{i}\hbar\left(\frac{\partial}{\partial z}\right)_{\text{ph}} |\phi\rangle \tag{4.1}$$

and to

$$P|\phi\rangle = \mathrm{i}\hbar\left(y\frac{\partial}{\partial z} - z\frac{\partial}{\partial y}\right)_{\text{ph}} |\phi\rangle \tag{4.2}$$

determine the translational mass in the z direction, M_z, and the rotational mass (moment of inertia), θ_x, for rotations about the x axis, respectively. The linear response operators are determined by starting from the linear response equation

$$[H, Q]_{\text{ph}} |\phi\rangle = -(\mathrm{i}\hbar/M)P|\phi\rangle, \tag{4.3}$$

with the boundary condition

$$\langle\phi| [Q, P] |\phi\rangle = \mathrm{i}\hbar \tag{4.4}$$

and M being the inertia parameter associated to the collective motion described by q. The objective is to find for a given 1p–1h and 1h–1p operator P (time odd) a 1p–1h operator Q (time even) that solves (4.3). It is convenient to introduce a

time-even 1p–1h and 1h–1p operator R by

$$R\,|\phi\rangle = MQ\,|\phi\rangle. \tag{4.5}$$

Equation (4.3) transforms to

$$[H, R]_{\text{ph}}\,|\phi\rangle = -\mathrm{i}\hbar P\,|\phi\rangle. \tag{4.6}$$

The evaluation of the commutator is

$$[H, R]\,|\phi\rangle = [W_0, R]\,|\phi\rangle + W_R\,|\phi\rangle \tag{4.7}$$

where W_0 is the Hartree–Fock Hamiltonian and W_R is given by

$$W_R = \mathrm{Tr}\{[R, \rho_0]v\} \tag{4.8}$$

with the two-body interaction v. Then the linear response equation is solved by iteration

$$R^{(n+1)}\,|\phi\rangle = R^{(n)}\,|\phi\rangle - \varepsilon\{[H, R^{(n)}]_{\text{ph}} + \mathrm{i}\hbar P\}\,|\phi\rangle. \tag{4.9}$$

It is recommended that we take as starting operator for the iteration

$$R^{(0)}\,|\phi\rangle = -\mathrm{i}\hbar P\,|\phi\rangle. \tag{4.10}$$

The iteration procedure stops when $R^{(n+1)}\,|\phi\rangle = R^{(n)}\,|\phi\rangle$. This means that $R^{(n)}$ fulfils (4.6) and is linear response operator to P. The corresponding linear response mass can be obtained from (2.23) and (4.5) as

$$\hbar^2 M = \langle\phi|\,[R, [H, R]]\,|\phi\rangle = \mathrm{i}\hbar\,\langle\phi|\,[P, R]\,|\phi\rangle. \tag{4.11}$$

The corresponding GCM mass parameters can be evaluated by inserting the operators P into (2.7). Although (2.7) is written in terms of double anticommutators, it can equivalently be transformed to an expression in terms of double commutators such that the same code can be used, which evaluates the mass parameter of (4.11). Since P is a time-odd and Hermitian 1p–1h and 1h–1p operator with respect to $|\phi\rangle$ it can be represented by

$$P = \mathrm{i}\sum_{nj} p_{nj}(a_n^+ a_j - a_j^+ a_n) \tag{4.12a}$$

with some real coefficients p_{nj}, where n indicates particle states with respect to $|\phi\rangle$, and j the corresponding hole states. We can formulate an operator $\tilde{Q}$, so-called 'locally redundant' to P (see Goeke and Reinhard 1980), as

$$\tilde{Q} = \sum_{nj} p_{nj}(a_n^+ a_j + a_j^+ a_n). \tag{4.12b}$$

Apparently, one has

$$\tilde{Q}\,|\phi\rangle = \sum_{nj} p_{nj} a_n^+ a_j\,|\phi\rangle = -\mathrm{i}P\,|\phi\rangle \tag{4.12c}$$

$$\langle\phi|\,\tilde{Q} = \sum_{nj} p_{nj}\,\langle\phi|\,a_j^+ a_n = +\mathrm{i}\langle\phi|\,P. \tag{4.12d}$$

One should note that (4.12*c*) and (4.12*d*) are only true since the operators P and $\tilde{Q}$ are acting on the Slater determinants $|\phi\rangle$, whose particle and hole states they are constructed from. (There is obviously no relation $\tilde{Q} = -\mathrm{i}P$.) Using (4.12) an

elementary and straightforward calculation shows without further assumptions that

$$\langle\phi|\,P^2\,|\phi\rangle = \langle\phi|\,\tilde{Q}^2\,|\phi\rangle$$

and

$$\langle\phi|\,\{P,\{\tilde{H},P\}\}\,|\phi\rangle = \langle\phi|\,[\tilde{Q},[H,\tilde{Q}]]\,|\phi\rangle.$$

With the help of these formulae, (2.7) transforms to

$$\frac{1}{M^{\mathrm{GCM}}} = \frac{\langle\phi|\,[\tilde{Q},[H,\tilde{Q}]]\,|\phi\rangle}{4\langle\phi|\,\tilde{Q}^2\,|\phi\rangle^2}. \tag{4.13}$$

The evaluation of the double commutator gives

$$\langle\phi|\,[\tilde{Q},[H,\tilde{Q}]]\,|\phi\rangle = \langle\phi|\,[\tilde{Q},[W_0,\tilde{Q}]]\,|\phi\rangle + \langle\phi|\,[\tilde{Q},W_{\tilde{Q}}]\,|\phi\rangle. \tag{4.14}$$

$W_{\tilde{Q}}$ is given in analogy to (4.8): $W_{\tilde{Q}} = \mathrm{Tr}\{[\tilde{Q},\rho_0]v\}$. The second term in (4.14) can be transformed to

$$\langle\phi|\,[\tilde{Q},W_{\tilde{Q}}]\,|\phi\rangle = \mathrm{Tr}\{\mathrm{Tr}\{[\tilde{Q},\rho_0]v\}[\tilde{Q},\rho_0]\} \tag{4.15}$$

which for the Skyrme interaction yields (see the appendix)

$$\mathrm{Tr}\{\mathrm{Tr}\{[\tilde{Q},\rho_0]v\}[\tilde{Q},\rho_0]\} = -\frac{(3t_1+5t_2)}{32}\int \mathrm{d}^3r j_{\tilde{Q}}^2(\boldsymbol{r}) \tag{4.16}$$

with

$$\boldsymbol{j}_{\tilde{Q}}(\boldsymbol{r}) = [(\boldsymbol{\nabla}-\boldsymbol{\nabla}')\rho_{\tilde{Q}}(\boldsymbol{r},\boldsymbol{r}')]_{\boldsymbol{r}=\boldsymbol{r}'}. \tag{4.17}$$

The density $\rho_{\tilde{Q}}$ is given by

$$\rho_{\tilde{Q}} = \sum_{\alpha=1}^{A}\{\tilde{Q}\,|\alpha\rangle\langle\alpha| - |\alpha\rangle\langle\alpha|\,\tilde{Q}\}. \tag{4.18}$$

This is a generalisation of the density ρ_1 (3.10) and of the current $\boldsymbol{j}(\boldsymbol{r})$ (3.9) for a general time-even 1p–1h and 1h–1p operator $\tilde{Q}$. The final expression for the GCM mass parameter calculated with the Skyrme interactions then becomes

$$\frac{1}{M^{\mathrm{GCM}}} = \frac{\langle\phi|\,[\tilde{Q},[W_0,\tilde{Q}]]\,|\phi\rangle - (3t_1+5t_2)/32\int \mathrm{d}^3r j_{\tilde{Q}}^2(\boldsymbol{r})}{4\langle\phi|\,\tilde{Q}^2\,|\phi\rangle^2}. \tag{4.19}$$

5. Numerical methods

The Slater determinants $|\phi_q\rangle$ are treated numerically by handling the set of occupied single-particle states $\{|\alpha,n\rangle,\ \alpha=1,\ldots,A\}$. They are represented on a three-dimensional grid in coordinate and momentum space

$$\alpha(\boldsymbol{r}) = \langle\boldsymbol{r}\,|\,\alpha\rangle \tag{5.1}$$

$$\alpha(\boldsymbol{k}) = \langle\boldsymbol{k}\,|\,\alpha\rangle. \tag{5.2}$$

A single-particle operator S is handled by its action on the states $|\alpha,n\rangle$. The states $S\,|\alpha,n\rangle$ are then also represented in coordinate and momentum space.

For the wavefunctions we assumed quartet symmetry. This means that protons and neutrons are treated in the same way assuming an effective charge $\frac{1}{2}e$. We use

reflection symmetries with respect to the xz and yz plane. The grid in coordinate space consists of $16 \times 16 \times 32$ mesh points. The spacing Δ between the mesh points had to be chosen according to the required accuracy. For the calculation of ^{12}C–^{20}Ne with SK V and ^{16}O–^{16}O with SK M* a Δ of 1.0 fm was giving satisfactory results; for the calculations of ^{12}C–^{20}Ne with SK III and SK BKN a Δ of 0.8 fm was necessary.

The transformation between coordinate and momentum space is performed by fast Fourier techniques. For interactions of the Skyrme type Fourier components of the wavefunction with an energy $\hbar^2k^2/2m$ higher than $E_{\mathrm{CUT}} = 100$–200 MeV are no longer to be considered as physical. We can therefore assume that all Fourier components corresponding to energies larger than E_{CUT} are zero. This reduces considerably the number of mesh points in the momentum grid. The E_{CUT} was chosen according to $E_{\mathrm{CUT}} = 100$ MeV and 160 MeV for $\Delta = 1.0$ fm and $\Delta = 0.8$ fm, respectively.

In order to obtain stability the stepsize ε in the evaluation of the GRAD path (2.4), (3.1) and of the ATDHF (2.27), (3.2) has to be chosen such that

$$\varepsilon_{\mathrm{G}} \leqslant 2/E_{\mathrm{CUT}} \tag{5.3a}$$

for the GRAD path, and

$$\varepsilon_{\mathrm{A}} \leqslant 2/E_{\mathrm{CUT}}E_{\mathrm{CUT}} \tag{5.3b}$$

for the ATDHF path, showing that the iteration for the ATDHF path needs a much smaller stepsize ε as the iteration for the GRAD path and needs therefore an order of magnitude more computation time.

The speed of iteration for solving the linear response equation can be enhanced by introducing a damping factor

$$\varepsilon \rightarrow \varepsilon'(k) = \frac{\delta}{(\hbar^2k^2/2m) + C}\,\varepsilon_{\mathrm{G,A}} \tag{5.4}$$

and by incorporating norm stabilisation (Reinhard *et al* 1984)

$$N^{(n)} = \frac{\langle \phi_q | P^2 | \phi_q \rangle}{-\mathrm{i}\langle \phi_q | P^+[H, R^{(n)}] | \phi_q \rangle}. \tag{5.5}$$

Then the iteration equation for the linear response mass reads in terms of the single-particle wavefunctions

$$R^{(n+1)} |\alpha\rangle = N^{(n)}R^{(n)} |\alpha\rangle - \varepsilon'(k)\{N^{(n)}[H, R^{(n)}]_{\mathrm{ph}} + \mathrm{i}P\} |\alpha\rangle. \tag{5.6}$$

Particles and holes are defined with respect to $|\phi_q\rangle$ or its single-particle states $|\alpha\rangle$. The energy-dependent stepsize $\varepsilon'(k)$ equalises the different speed of convergence of the different single-particle wavefunctions, in order that all components converge with nearly the same speed (Reinhard and Cusson 1982). The parameters δ and C have to be adjusted in a way to give a fast and stable convergence. The actual values of δ and C depend on the system and on the interaction and are given together with the grid parameters in tables 2 and 3.

For the explicit evaluation of the ATDHF mass along the gradient path the operator $\partial/\partial q$ is approximated by

$$\frac{\partial}{\partial q} |\phi_q\rangle = \frac{|\phi_q + \delta_q\rangle - |\phi_q\rangle}{\delta_q}. \tag{5.7}$$

Table 2. Parameters for the evaluation of the ATDHF path.

	ε (MeV^{-2})	E_{CUT} (MeV)	Δ (fm)	δ (MeV)	C (MeV)
^{12}C–^{20}Ne, SK III	5×10^{-5}	160	0.8	1.6	30
^{12}C–^{20}Ne, SK V	5×10^{-5}	100	1.0	3.5	190
^{16}O–^{16}O, SK M*	10^{-4}	100	1.0	1.5	30

Table 3. Parameters for the evaluation of the GRAD path.

	ε (MeV^{-1})	E_{CUT} (MeV)	Δ (fm)	δ (MeV)	C (MeV)
^{12}C–^{20}Ne, SK III	5×10^{-3}	160	0.8	1.6	30
^{12}C–^{20}Ne, SK V	10^{-2}	100	1.0	0.9	30

The size of δ_q influences considerably the accuracy of the results for the collective ATDHF mass. To check this we calculated the ATDHF mass at different points on the ATDHF path with two distinct methods: with the ATDHF method (2.23) and with the linear response method (4.11) by inserting (5.7) as starting operator for $R(0)$. The result is shown in figure 1. The horizontal line indicates the value for the collective mass as calculated with the ATDHF method. The iterated ATDHF mass calculated with the linear response method reaches for small δ_q exactly the value of the mass calculated with the ATDHF method. The mass parameters can be checked in the asymptotic region where the collective mass of the relative motion is given by the reduced mass μ of the system. It turns out that the conventional ATDHF way to evaluate the collective mass $M(q)$ is more sensitive to the value of E_{CUT} and the limitation of the grid than the linear response method. For example, in the asymptotic region of the ^{12}C–^{20}Ne system the deviation of the ATDHF mass from the reduced mass are $\leqslant 4\%$ and those of the linear response mass are $\leqslant 0.1\%$. For a pair of doubly closed shell nuclei, as e.g., ^{16}O–^{16}O both methods work equally well. In the present calculation the linear response method has been taken to obtain the proper asymptotic mass.

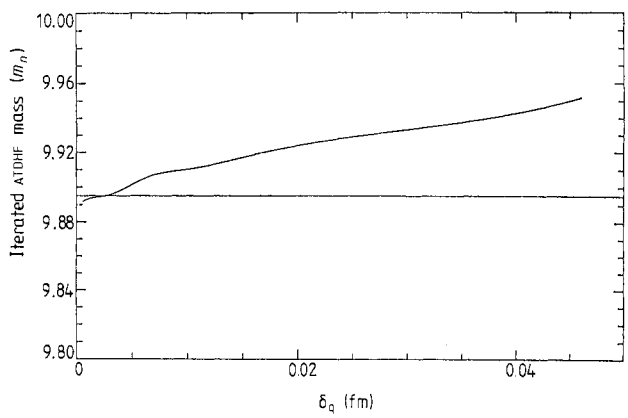

Figure 1. Collective mass in linear response theory as a function of δ_q. The horizontal line indicates the corresponding ATDHF mass. Skyrme III force. ATDHF path.

After a suitable labelling of the Slater determinants the collective potentials, mass parameters, etc. can easily be extracted from the collective path. The labelling is done by means of a measuring operator D

$$q_n = \langle \phi_n | D | \phi_n \rangle. \tag{5.8}$$

The choice of the operator D is purely a matter of convenience. For heavy-ion collisions a reasonable labelling is given by a coordinate which is identical to the cluster distance in the asymptotic region. Such a coordinate will be denoted by R and can be extracted from the $|\phi_n\rangle$ by

$$2\mu R^2 = \langle \phi_n | r^2 Y_{20} | \phi_n \rangle - Q_1 - Q_2 \tag{5.9}$$

where Q_1 and Q_2 are the quadrupole moments of the fragments along the collision axis. Since the coordinate R is extracted from the quadrupole moments of the system we call it the 'quadrupole distance'.

6. Application: the ^{12}C–^{20}Ne system as a test case

The ^{12}C–^{20}Ne system has been chosen because it represents a rather general case due to its deformed non-closed shells and because it allows to investigate the importance of transfer channels in fusion reactions (see Gissler *et al* 1986). We consider the configuration of the system as given in figure 2, i.e. an axial collision.

6.1. The collective path and the mass parameters

Figures 3 and 4 show the collective potential $V(R)$ calculated along the gradient and ATDHF paths as a function of the quadrupole distance for the ^{12}C–^{20}Ne system with the interactions SK III and SK V. In the overlap region to the left of the saddle point (at a distance of about 9 fm) there are considerable differences between gradient and ATDHF path. This effect is more accentuated for SK III than for SK V. By approaching the Hartree–Fock point at about 4.8 fm these differences disappear of course and the two potentials become identical. As can be seen in figure 3 the potential of the ^{12}C–^{20}Ne system is in this part of the path also identical to the potential of the ^{16}O–^{16}O system. The gradual change of the ^{12}C–^{20}Ne configuration to a ^{16}O–^{16}O one is an indication for an α transfer. The importance of

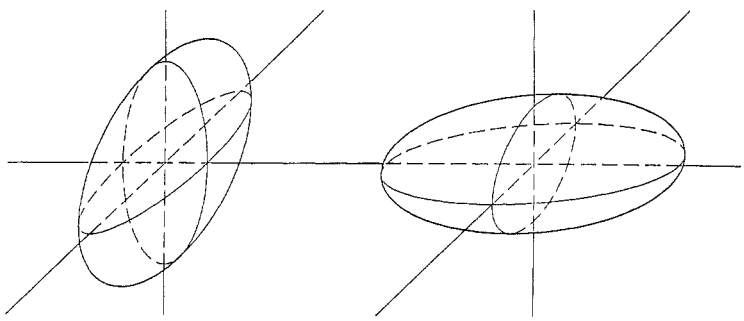

Figure 2. Axially symmetric configuration of the ^{12}C–^{20}Ne system.

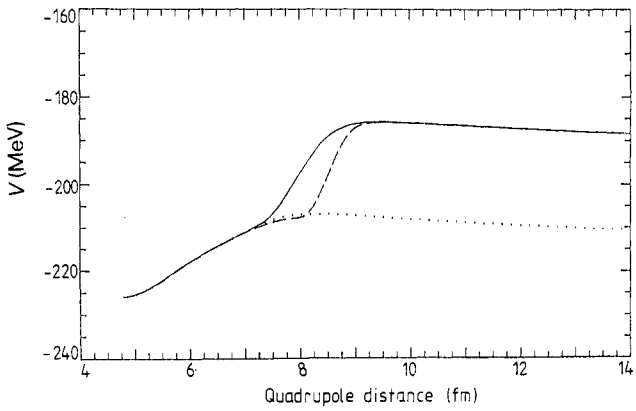

Figure 3. Classical potential $V(R)$ of the ^{12}C–^{20}Ne system calculated with the Skyrme III force along the ATDHF path (full curve) and along the GRAD path (broken curve). The dotted curve shows the potential $V(R)$ for the ^{16}O–^{16}O system obtained with the Skyrme III force.

this α transfer and its physical implications to subbarrier fusion processes have been discussed in Gissler *et al* (1986) and Reinhard and Goeke (1987).

A region where such clear changes of the structure like an α transfer takes place is well suited to check the various prescriptions for the evaluation of the collective path and of the collective mass parameters. The collective mass parameter can be evaluated in four different ways: (i) ATDHF path with ATDHF mass. (ii) ATDHF path with GCM mass. (iii) GRAD path with ATDHF mass. (iv) GRAD path with GCM mass. Figures 5 and 6 show $M(R)$ for the ^{12}C–^{20}Ne system calculated with SK III and SK V. In figures 7 and 8 the ratio of the ATDHF mass to the GCM mass is plotted. For the collective mass the differences between the various methods are quite remarkable. Along the same path the ATDHF mass may differ by a factor of two and the same mass along different paths shows deviations of the order of a factor four. Similar effects hold for the translational and rotational inertia parameters. There the differences amount to about 50%. These numbers are to be contrasted with the accuracy of ATDHF reproducing the asymptotic values: translational mass in the z

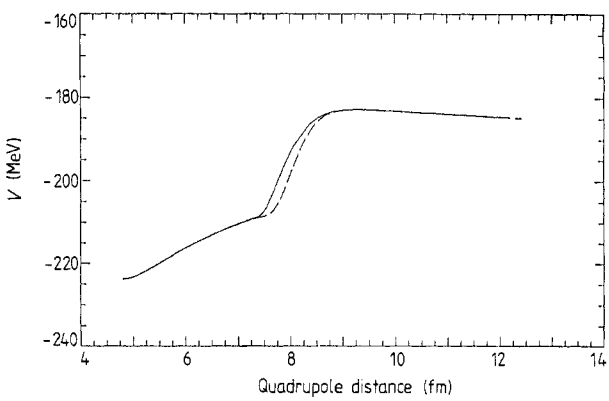

Figure 4. Classical potential $V(R)$ of the ^{12}C–^{20}Ne system calculated with Skyrme V force along the ATDHF path (full curve) and along the GRAD path (broken curve).

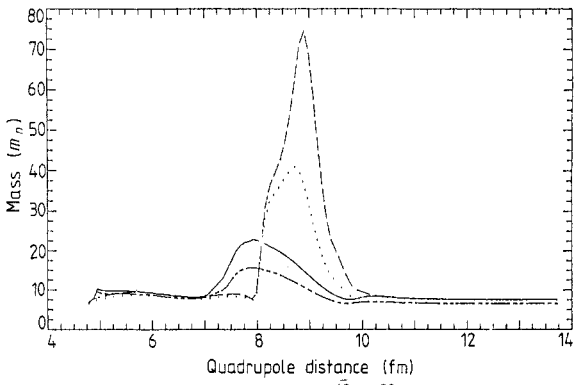

Figure 5. Collective mass for the ^{12}C–^{20}Ne system in ATDHF and GCM approximation along the ATDHF and GRAD path calculated with the Skyrme III force. (————, ATDHF path with ATDHF mass; — — — — —, ATDHF path with GCM mass; - - - - -, GRAD path with ATDHF mass; . . . . . , GRAD path with GCM mass).

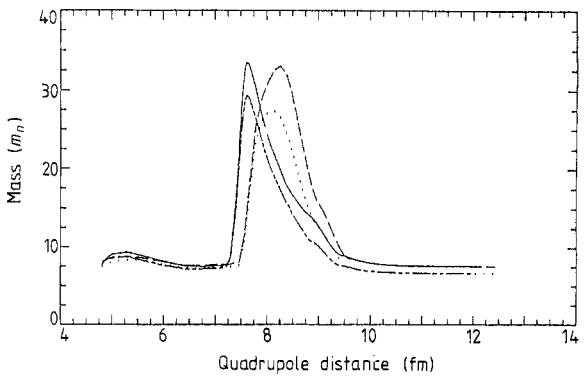

Figure 6. Same as figure 5 but for the Skyrme V interaction.

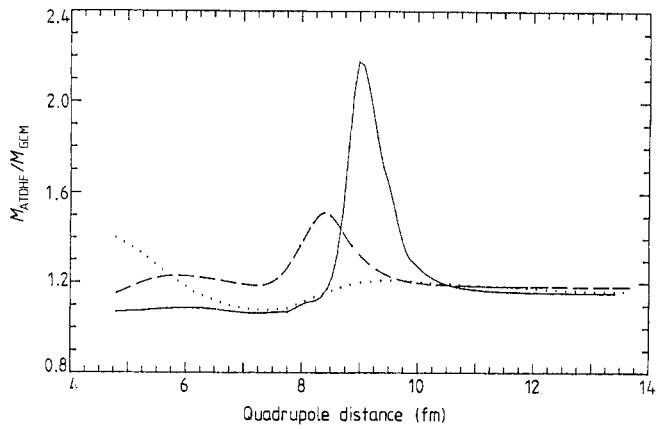

Figure 7. Ratio of ATDHF and GCM mass for the collective mass M (full curve), the translational mass in the z direction M_z (broken curve) and moment of inertia θ_x (dotted curve) for the ^{12}C–^{20}Ne system calculated with the Skyrme III force. The collective mass M is evaluated along the GRAD path, M_z and θ_x are evaluated along the ATDHF path.

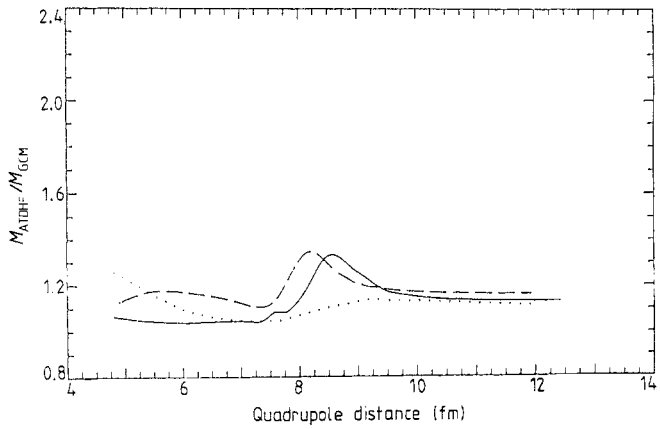

Figure 8. Same as figure 7 but for the Skyrme V interaction.

direction by $\leqslant 0.2\%$, translational mass in the x direction by $\simeq 1\%$ and the collective ATDHF mass of the relative motion agrees with the reduced mass to better than $\simeq 0.5\%$. The values for the corresponding GCM mass parameter are $\simeq 15\%$, $\simeq 5\%$ and $\simeq 12\%$ respectively.

From these numbers one can draw some simple conclusions. Along a given path the ATDHF masses are preferable since they are asymptotically correct and the simpler GCM mass parameter does not appear to be a reliable good approximation.

When transforming to the reduced coordinate (see Provoost *et al* 1984) the changes of the collective mass are included in the potential. The potential $V(R)$ including the quantum corrections $Z(R)$ is shown in figures 9 and 10 as a function of the reduced distance for the ATDHF and GRAD path with the various mass evaluation methods. The potentials contain the full information of the system but are not observable quantities. For a proper evaluation of the various methods used we will therefore calculate the astrophysical S-factor of the $^{12}C + {}^{20}Ne \rightarrow {}^{32}S$ fusion in the next subsection.

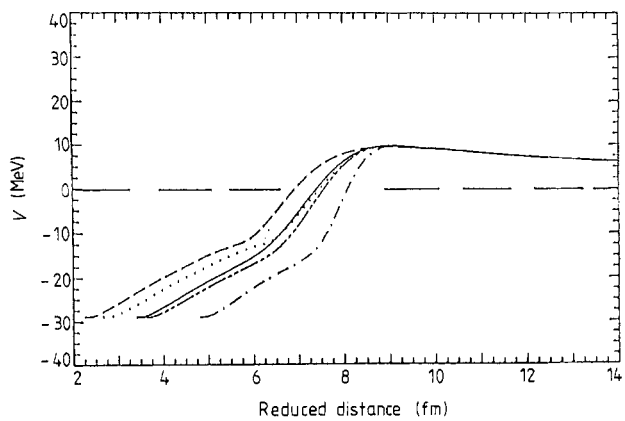

Figure 9. Quantum-corrected potential $V(\bar{R}) - Z(\bar{R})$ as a function of the reduced distance $\bar{R}$ for the ^{12}C–^{20}Ne system calculated with the Skyrme III interaction for the different combinations of path and mass evaluation methods. (————, ATDHF path with ATDHF mass; — — — —, ATDHF path with GCM mass; — · — · —, ATDHF path with constant mass; – – – –, GRAD path with ATDHF mass; . . . . . , GRAD path with GCM mass.)

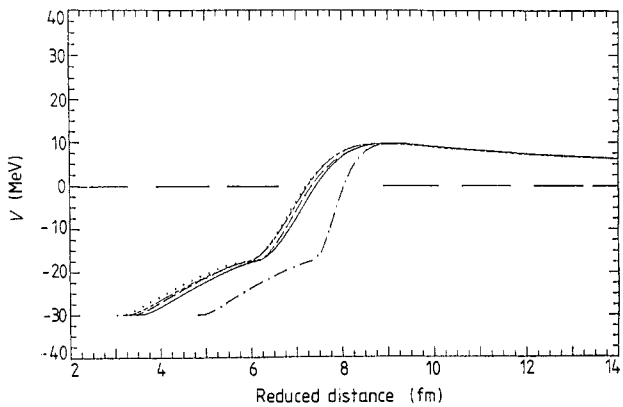

Figure 10. Same as in figure 9 but for the Skyrme V interaction. The line types for the different path and mass evolution methods are those of figure 9.

Actually the difference between GCM and quantised ATDHF is not always as large as in the given $^{12}C + {}^{20}Ne \rightarrow {}^{32}S$ example. Calculations for the $\alpha + \alpha$, ^{16}O–^{16}O and ^{40}Ca–^{40}Ca systems show that for doubly closed fragments the GCM is a good approximation to quantised ATDHF. This can be explicitly seen at figures 11 and 12, where the potentials and masses for the ^{16}O–^{16}O system are given.

6.2. Subbarrier fusion for the $^{12}C + {}^{20}Ne \rightarrow {}^{32}S$ system

After the evaluation of the potential $V(R)$, the collective mass parameter $M(R)$, the quantum corrections $Z(R)$ and of the translational and rotational moments of inertia we can determine the collective Hamiltonian H_c. Then we can extract from H_c the subbarrier fusion cross section (Goeke *et al* 1983).

The transmission coefficients are evaluated approximately by generalised WKB methods

$$T_L(E_{CM}) = [1 + \exp(2I_L)]^{-1} \tag{6.1}$$

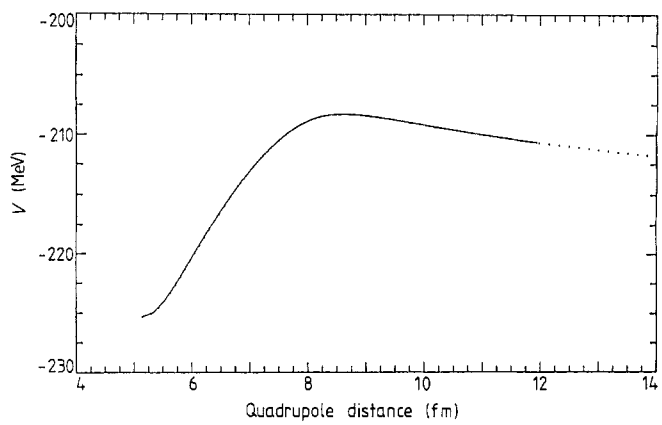

Figure 11. Classical potential $V(R)$ for the ^{16}O–^{16}O system calculated with the Skyrme M* force along the ATDHF path (full curve) and along the GRAD path (dotted curve).

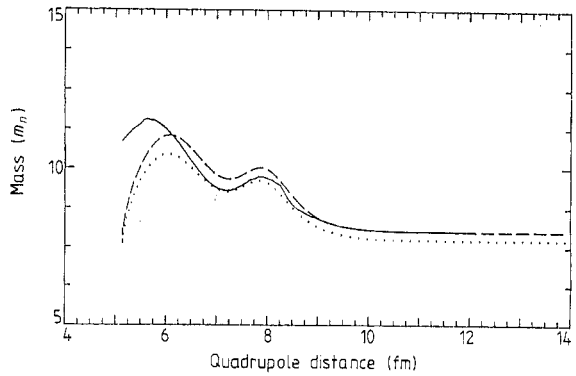

Figure 12. Collective mass for the ^{16}O–^{16}O system calculated with the Skyrme M* force: ATDHF mass along the ATDHF path (full curve), ATDHF mass along the GRAD path (broken curve) and GCM mass along the GRAD path (dotted curve).

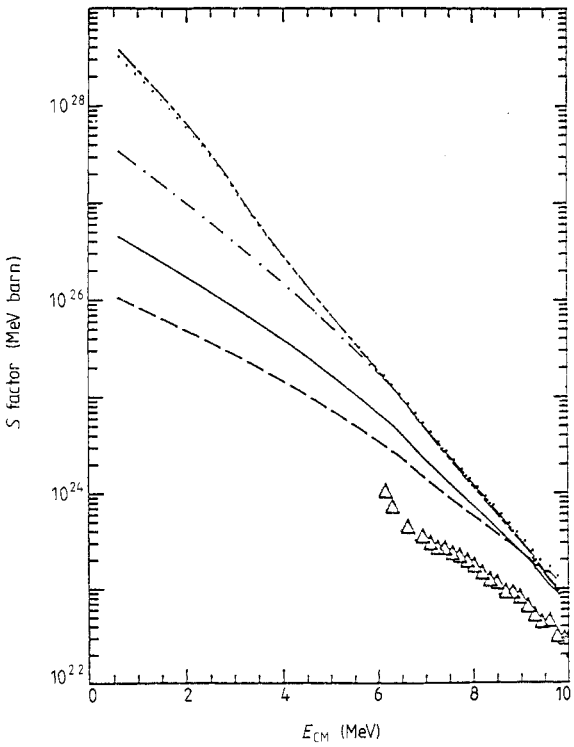

Figure 13. Astrophysical S factor for the subbarrier fusion of the ^{12}C–$^{20}Ne \rightarrow {}^{32}S$ system calculated with the Skyrme III interaction. The experimental values are from Hulke *et al* 1980. (————, ATDHF path with ATDHF mass; — — — —, ATDHF path with GCM mass; —·—·—, ATDHF path with constant mass; – – – –, GRAD path with ATDHF mass; . . . . . , GRAD path with GCM mass.)

with

$$I_L(E_{CM}) = \int_{R_a}^{R_b} dR \left[\frac{2M(R)}{\hbar^2} \left(V(R) - Z(R) + \frac{\hbar^2}{2\theta(R)} L(L+1) - E_{CM} \right) \right]^{1/2} \tag{6.2}$$

where R_a and R_b are the classical turning points of the quantum mechanical potential $V(R) - Z(R)$ including the centrifugal term. Then the total fusion cross section is given by

$$\sigma_{FUS}(E_{CM}) = \frac{\pi\hbar^2}{2\mu E_{CM}} \sum_L (2L+1) T_L(E_{CM}). \tag{6.3}$$

Instead of σ_{FUS} it is preferable to refer to the astrophysical S-factor defined by

$$S(E_{CM}) = E_{CM}\sigma_{FUS}(E_{CM}) \exp(2\pi Z_1 Z_2 e^2/\hbar v) \tag{6.4}$$

where v is the relative velocity of the ions.

Figures 13 and 14 show the astrophysical S-factor of the $^{12}C + {}^{20}Ne \rightarrow {}^{32}S$ system calculated with the interactions SK III and SK V. The calculations are performed for the ATDHF and for the GRAD path with the various evaluations of the collective mass parameter. The transitional and rotational moments of inertia, needed for the quantum corrections, are calculated in Thouless–Valatin theory. In the energy region, where experimental data are available, all curves show systematic deviations

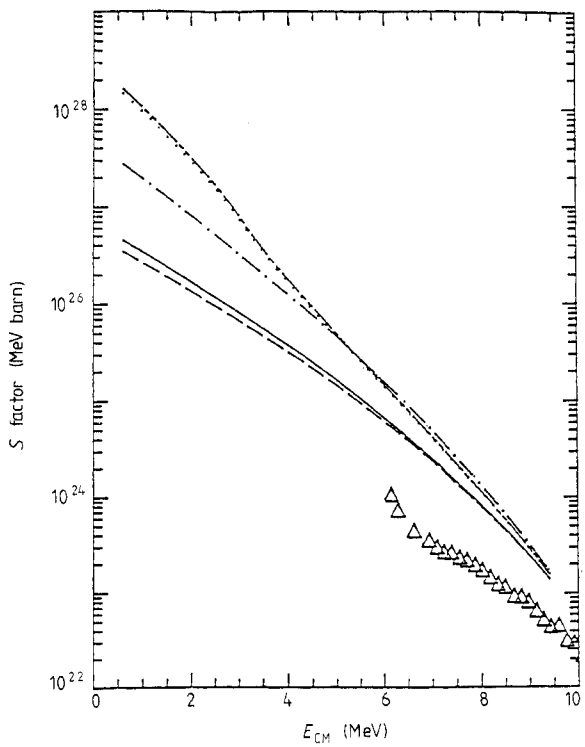

Figure 14. Astrophysical S factor for the subbarrier fusion of the $^{12}C + {}^{20}Ne \rightarrow {}^{32}S$ system calculated with the Skyrme V interaction. (————, ATDHF path with ATDHF mass; — — — —, ATDHF path with GCM mass; —·—·—, ATDHF path with constant mass; – – – –, GRAD path with ATDHF mass; . . . . . , GRAD path with GCM mass.)

from the data of about half an order of magnitude. This can probably be improved by use of a better interaction and of coupled channel techniques with angular momentum projection. However, the point relevant for the present considerations is that at smaller energies of about $E_{CM} = 1$ MeV the differences between the various methods amount to three orders of magnitude in the astrophysical S-factor. Thus, strictly speaking, in this situation one is bound to use the most general of the methods, i.e. ATDHF path combined with the ATDHF mass.

However, one can learn from figures 13 and 14 that the GRAD path together with the ATDHF mass seems to be a reasonable approximation, which in the case of the Skyrme V interaction even works rather well. On the other hand the methods which approximate the mass rather than the path produce, particularly in the low energy region, rather strong deviations from the ATDHF values.

We would like to stress that these conclusions are not made by comparison with the data. From that one would conclude even that the GRAD path with the ATDHF mass would be the best way to describe the fusion cross section. This, however, would be wrong since an approximation can only be correct by chance if the method, which it approximates, is inaccurate. The data are basically only used to show that the theories are not so far wrong that any conclusion from them would be immaterial. After noticing this, the conclusions are based solely on the comparison of the theories with each other and the conclusion is very simple: GCM is not a good approximation to quantised ATDHF.

7. Conclusions

In the present paper we perform a numerical comparison between the quantised ATDHF theory and the generator coordinate approach (GCM). The comparison is performed by considering two collective paths, the ATDHF path and the GRAD path (derivable by GCM) together with the ATDHF mass and the GCM mass for relative motion of two heavy ions. In order to study a rather general case, the collision of two non-closed shell nuclei is considered as a practical example: $^{12}C + {}^{20}Ne \rightarrow {}^{32}S$.

The mass parameters turn out to be rather sensitive quantities. Along the same path the ATDHF mass and GCM mass of relative motion differ up to a factor of two, the same mass along different paths up to a factor of four. For the translational and rotational moments of inertia the deviation between the GCM and ATDHF values differ in the overlapping region by up to 50%.

It is shown that the subbarrier fusion cross section at low energies shows, due to the different paths and masses, deviations up to three orders of magnitude. For open shell fragments it is therefore concluded that the use of the simpler GCM method as an approximation to quantised ATDHF is generally not justified. In particular the GCM approximation to the collective mass turns out to be unreliable. Replacing the ATDHF path by the GRAD path might be considered as tolerable.

Acknowledgments

This work was supported in part by the Bundesministerium für Forschung und Technologie (Intern. Büro, Karlsruhe) and the Bulgarian Committee of Sciences (contract no 802).

Appendix A

Equation (4.15) can be transformed to

$$\mathrm{Tr}\{\mathrm{Tr}\{[\tilde{Q}, \rho_0]v\}[\tilde{Q}, \rho_0]\} = \mathrm{Tr}\,\mathrm{Tr}\{\rho_{\tilde{Q}} v \rho_{\tilde{Q}}\} \tag{A1}$$

where $\rho_{\tilde{Q}}$ is given by

$$\rho_{\tilde{Q}} = [\tilde{Q}, \rho_0]. \tag{A2}$$

The RHS expression of (A1) represents (up to a factor of two) the contribution of the density $\rho_{\tilde{Q}}$ to the Hartree–Fock energy. For the Skyrme interaction the Hartree–Fock energy is given by

$$E = \int \mathrm{d}^3 r H(\boldsymbol{r}) = \int \mathrm{d}^3 r \Big(\frac{\hbar^2}{2m} \tau(\boldsymbol{r}) + \tfrac{3}{8} t_0 \rho^2(\boldsymbol{r}) + \frac{(3t_1 + 5t_2)}{16} [\rho(\boldsymbol{r})\tau(\boldsymbol{r}) - \boldsymbol{j}^2(\boldsymbol{r})] - \frac{(9t_1 - 5t_2)}{64} \rho(\boldsymbol{r}) \nabla^2 \rho(\boldsymbol{r}) + \tfrac{1}{16} t_3 \rho^{2+\alpha}(\boldsymbol{r}) + H_{\mathrm{Coul}}(\boldsymbol{r}) \Big) \tag{A3}$$

The only contribution to E depending on $\rho_{\tilde{Q}}$ is the term proportional to $\boldsymbol{j}^2_{\tilde{Q}}(\boldsymbol{r})$. This means

$$\mathrm{Tr}\,\mathrm{Tr}\{\rho_{\tilde{Q}} v \rho_{\tilde{Q}}\} = -\frac{(3t_1 + 5t_2)}{32} \int \mathrm{d}^3 r \boldsymbol{j}^2_{\tilde{Q}}(\boldsymbol{r}). \tag{A4}$$

References

Bartel J, Quentin P, Brack M, Guet C and Hakansson H B 1982 *Nucl. Phys.* A **386** 79
Beiner M, Flocard H, Nguyen Van Giai and Qentin P 1975 *Nucl. Phys. A* **238** 29
Bonche P, Koonin S and Negele J W 1976 *Phys. Rev. C* **13** 1226
Deumens E 1982 *PhD thesis* RUCA, Antwerp
Engel Y M, Brink D M, Goeke K, Krieger S J and Vautherin D 1975 *Nucl. Phys.* A **249** 215
Fiebig H R and Weiguny A 1976 *Z. Phys. A* **279** 275
Friedrich H 1981 *Phys. Rep.* **74** 209
Friedrich H, Huesken H and Weiguny A 1974 *Nucl. Phys. A* **220** 125
Gissler R, Provoost D, Gruemmer F and Goeke K 1986 *Phys. Lett.* **166B** 385
Goeke K, Gruemmer F and Reinhard P-G 1983 *Ann. Phys., NY* **150** 504
Goeke K and Reinhard P-G 1980 *Ann. Phys., NY* **124** 249
Griffin J J and Wheeler J A 1957 *Phys. Rev.* **108** 311
Hill D L and Wheeler J A 1953 *Phys. Rev.* **89** 1102
Hulke G, Rolfs C and Trautvetter H P 1980 *Z. Phys.* A **297** 161
Peierls R E and Yoccoz J 1957 *Proc. Phys. Soc.* A **70** 381
Provoost D, Gruemmer F, Goeke K and Reinhard P-G 1984 *Nucl. Phys.* A **431** 139
Reinhard P-G and Cusson R Y 1982 *Nucl. Phys.* A **378** 418
Reinhard P-G and Goeke K 1979 *Phys. Rev.* C **20** 1546
——, 1987 *Rep. Prog. Phys.* **50** 1
Reinhard P-G, Gruemmer F and Goeke K 1984 *Z. Phys.* A **317** 339
Ring R and Schuck P 1980 *The Nuclear Many Body Problem* (Berlin: Springer)
Slavov B, Dimitrov V I, Goeke K, Gruemmer F and Reinhard P-G 1986 *Nucl. Phys.* A **454** 392
Thouless D J and Valatin J G 1962 *Nucl. Phys.* **31** 211